17th World Conference on Earthquake Engineering, 17WCEE
Sendai, Japan - September 13th to 18th 2020

STEEL DOUBLE-HSS MEMBERS FOR SEISMIC FORCE-RESISTING SYSTEMS

S.-H. Chao[(1)], K. Park [(2)], C. Jiansinlapadamrong [(3)], B. Price[(4)]

[(1)] Professor, The University of Texas at Arlington, shchao@uta.edu
[(2)] Post-doc Research Fellow, The University of Texas at Arlington, 1817ms@gmail.com
[(3)] Project Engineer, AG&E, chad_a2@hotmail.com
(4) Project Engineer, Martinez Moore Engineers, bprice@martinezmooreengineers.com

Abstract

This paper presents an experimental investigation on the applications of the steel double hollow structural section (double-HSS) for seismic resistant members, including moment connections in special moment frames (SMFs), shear links in eccentrically braced frames (EBFs), and chord members in special truss moment frames (STMFs). Hollow structural sections (HSSs) are highly efficient and are used in resisting compression, torsion, and bending. Their high torsional rigidity generally eliminates lateral-torsional buckling (LTB), which also eliminates the need for lateral bracing in beam-type members. As a result, the plastic rotational capacity and strength degradation rate are mainly governed by flange local buckling (FLB) and web local buckling (WLB). The other advantages of using double-HSSs are: 1) They effectively reduce the width-thickness ratios (*b/t*) of the flanges and have a similar moment capacity equivalent to a single HSS thereby considerably increasing compactness and ductility under bending; 2) they provide simple and economic connection details, The gusset plate in-between the two webs also provides support for minimizing WLB; 3) the presence of a gusset plate relocates the plastic hinge away from the column face, which prevents large inelastic strains in the welds between the beam (or link) and the column; 4) they have high shear capacity due to four webs, 5) The welding requirement can be much less stringent since in general only fillet welds are needed. This paper provides experimental results of double-HSS moment connections in SMFs, double-HSS links in EBFs and double-HSS chord members in STMFs.

Keywords: Hollow Structural Section (HSS), Eccentrically Braced Frames, Moment Frames, Special Truss Moment Frames

1. Introduction

According to AISC 341–Seismic Provisions for Structural Steel Buildings [1], beam-to-column moment connections in a special moment frame (SMF) should maintain a flexural strength under cyclic rotations of at least $0.8M_p$ at a story drift angle of 0.04 rad. M_p is the nominal plastic flexural strength of the section. This required rotational capacity of 0.04 rad provides a safeguard against early strength degradation and, hence, potential frame instability due to P-Delta effects [1]. For a typical wide-flange beam, its rotational capacity is controlled by three major local instabilities: lateral-torsional buckling (LTB), flange local buckling (FLB), and web local buckling (WLB). These three local instabilities can occur simultaneously and strongly interact with each other [2]. Tests have shown how the interaction of these instabilities, all of which typically occur at the plastic hinge location of a beam, prevent a steel member from developing isotropic strain-hardening under subsequent large-amplitude cycles. For this reason, the member only develops a shorter plastic hinge length (which translates to less member deformation). Research results have also shown that the plastic rotational capacity and strength degradation rate can be strongly influenced by interactions between the three instabilities [3–5]. Despite LTB's negative effect on rotational capacity, it cannot be completely eliminated because AISC 341 [1] does not allow lateral bracing to be placed within the plastic hinge region (or the protected zone), which is the area where LTB typically occurs. In this regard, hollow structural sections (HSS) have a high torsional rigidity which generally prevents LTB, thereby eliminating the need for lateral bracing in flexural members. Consequently, the plastic rotational capacity and strength degradation rate are primarily governed by FLB and WLB.

Research on the behavior of hollow structural sections (HSSs) under large displacement reversals is limited. Fadden and McCormick [6, 7] conducted extensive pilot work and investigated the cyclic responses of single-HSS flexural members, with member sizes from HSS203.2×101.6×6.4 to HSS304.8×152.4×6.4. The fixed end of the single-HSS specimens was sandwiched between two large angles to provide a reusable connection, and stiffener plates were added to ensure that the inelastic deformation occurred outside of the connection region. As they pointed out, this beam-to-column configuration was for testing and was not a practical connection for a moment frame system. D'Aniello et al. [8] tested six single-HSS flexural members under either cyclic loading or monotonic loading. A heavily reinforced end connection with multiple stiffeners were also used in their specimens. Fadden and McCormick [6] found that maximum moments of single-HSS members occurred between rotations of 0.017 rad and 0.035 rad and their hysteretic behavior was significantly affected by flange and web local buckling, which led to a very quick degradation in moment capacity for some of the specimens. They concluded that larger width-thickness ratios (b/t) led to a more significant decrease in the moment capacity as well as rotational capacity due to the importance of the flange in resisting cyclic bending. Fadden and McCormick [6] also suggested that a b/t ratio below 25 and an h/t ratio below 40 are necessary to maintain 90% of the maximum moment strength at beam rotations of 0.04 rad. It is also noted that, in general, the beam-to-column connections for a single-HSS beams require more complicated detailing, as shown by Fadden and McCormick [7].

A new moment connection configuration consisting of a double-HSS welded to the column through a center gusset plate was investigated in this study (Fig. 1). The benefits of the proposed configuration are: First, an effective minimization of FLB without increasing the wall thickness is achieved by reducing the width-thickness ratio (b/t) using two HSSs [9], rather than a single-HSS (having equivalent moment capacity), thereby significantly enhancing the rotational ductility. Moreover, the gusset plate in-between the two webs provide support for minimizing WLB. Second, the double-HSS-gusset plate connection provides a simple but secure connection between the beam and column. Third, the configuration provides a greater rotation capacity compared to wide-flange sections. Fourth, the presence of a gusset plate relocates the plastic hinge away from the column face, which prevents large inelastic strains in the welds between the beam and column. The fifth benefit is the elimination of the need to use lateral support because LTB no longer exists for double-HSS flexural members.

This study also investigated a new double-HSS link (DHL) used as the link in eccentrically braced frames (EBFs) as shown in Fig. 2. DHL could considerably reduce the welding work while maintaining high

ductility under large displacement reversals. The proposed configuration consists of a double-HSS connected to braces or column flange through a center gusset plate secured by flare-bevel groove welds. In addition to the benefits discussed previously for double-HSS moment connections, additional advantages of using DHLs in EBFs are: 1) They provide simple and practical connection details between the beams and brace and the column; 2) typically, HSSs have an M_p/V_p ratio closer to 1.0 than wide-flange sections due to the fact that double-HSS sections have four webs which significantly increase the shear capacity. As a result DHLs can have a shorter length similar to a corresponding wide-flange shear yielding link while the yielding is still controlled by flexure, which eliminates the need for web stiffeners; 3) the welding requirement for DHLs is much less stringent than that of conventional EBFs since the double-HSS link does not require complete-joint-penetration (CJP) groove welds at the brace-beam connection nor any welding for stiffeners. In general, the only welds are flare-bevel groove welds and fillet welds if a DHL is connected to the column flange, and 5) the over-strength factor due to strain-hardening produced by flexural links is generally less than that produced by shear links leading to more economical designs for the elastic portion of the frame.

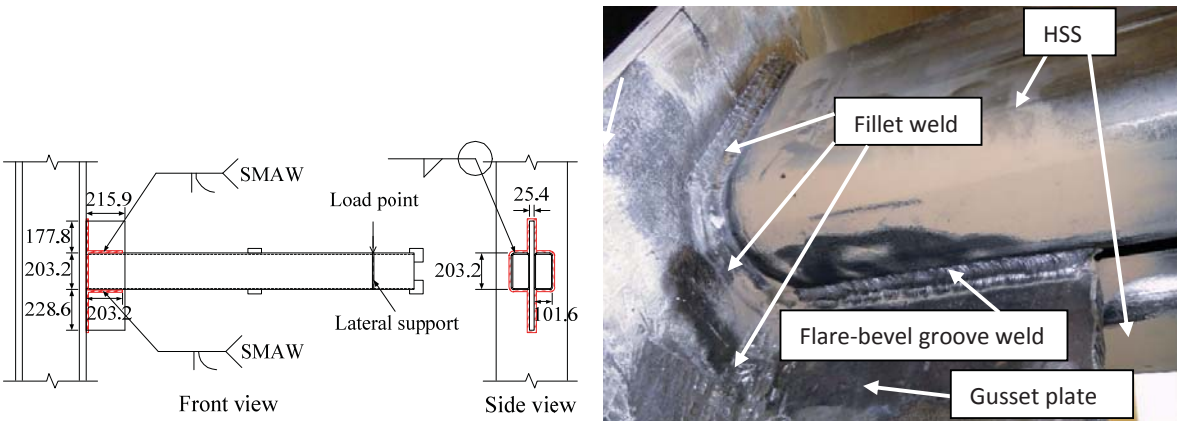

Fig. 1 – Proposed double-HSS connection for special moment frames: (a) cross-section and elevation views and (b) weld details at the end of the connection

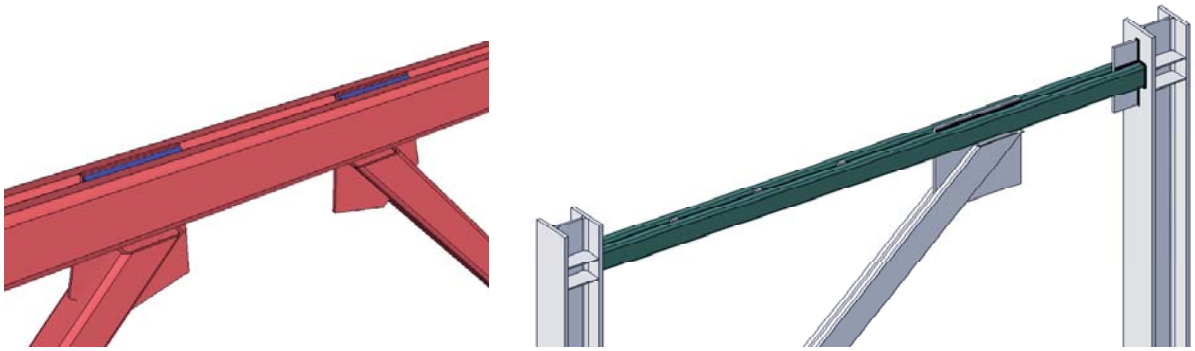

Fig. 2 –Double-HSS links for eccentrically braced frames

Steel special truss moment frames (STMFs) is one of the seismic force-resisting systems permitted by AISC 341 (Fig. 3). One major advantage to using the STMF system is that truss girders can be economically used over longer spans up to 20 m because greater overall lateral stiffness can be achieved by using deeper girders. In addition, the open webs can easily accommodate mechanical and electrical ductwork (Fig. 3). Therefore, this system offers a wide range of structural, architectural, and economical benefits because of its ability to achieve a large column-free floor. STMFs dissipate earthquake energy through the ductile chord

members of special segments located near the mid-span of the truss girders, which act as a structural "fuse" as shown in Fig. 3. Members outside of the special segment are designed to remain elastic, based on the gravity loads and expected maximum capacity of the chord members in the special segment. The energy dissipation capacity of a truss system can also be improved by using dissipative energy devices; for example, using short buckling-restrained braces in the special segments [10].

In contrast to moment frames in which the plastic rotational demand in beams is close to the story drift ratio, the plastic rotational demand of the chord members in a special segment of STMFs is significantly higher than the story drift ratio [11, 12]. For this reason, using double-HSS chord members can be a viable solution for providing greater inelastic rotational capacity due to the smaller *b*/*t* ratio of the flange and minimum impact by LTB.

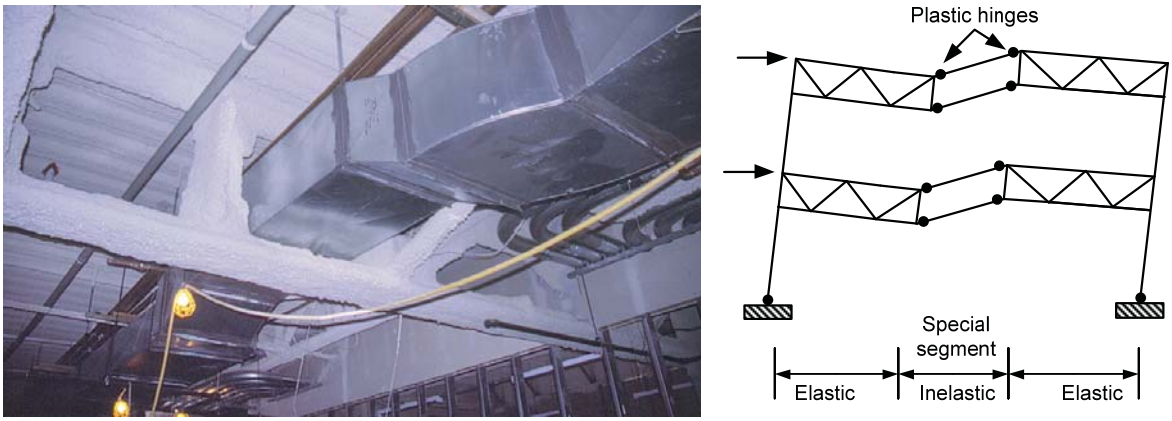

Fig. 3 –Steel special truss moment frames

Fig. 4 – Double-HSS truss members for special truss moment frames

2. Experimental Program and Results

2.1 Double-HSS Moment Connections

The test setup and test specimen, consisting of a single column with one cantilever beam, are illustrated in Figs. 1a and 5a. Lateral bracing was provided at the load application point as permitted by Section K2.2 of AISC 341 [1]. The two HSSs were welded to the center gusset plate by flare-bevel groove welds, whose size, $\frac{5}{8}\ t_{des}$ (= the effective throat), was determined according to the prequalified welded joint requirement in

Table 8-2 of AISC's Steel Construction Manual [13]. Fillet welds with a leg size of 12.7 mm and E70 electrode were used to connect the gusset plate and HSSs to the column's flange.

The double-HSS moment connection specimen presented in this paper was made of 2-HSS 203.2×101.6×12.7. The hysteresis response shown in Fig. 5b indicates that the strength did drop until the rotation reached 0.09-rad total member rotation (TMR, rad), which is calculated by dividing the vertical displacement measured at the loading point by the distance from the weld ends to the loading point. This rotation is equivalent to 0.068-rad story drift angle (SDA, rad) which is measured by the vertical displacement of the loading end of the specimen divided by the length from the middle of the column panel zone to the loading point. The maximum moment (average of positive and negative cycles) of this specimen occurred at approximately 0.045-rad SDA. The first sign of yielding was at 0.012-rad TMR or at 0.008-rad SDA based on the measurement of a strain gauge located on the flange near the corner where the HSS was welded to the gusset plate. During 0.013-rad SDA cycles, a crack tip at the weld ends was noticed but it did not propagate into the HSS. By 0.02-rad SDA, a flaking from the whitewash occurred and by 0.033-rad SDA, a crack had slightly propagated into the HSS. At 0.045-rad SDA (Fig. 5c), the fracture propagated slightly further, leading to a non-substantial strength loss. As the test continued to 0.055-rad SDA, fractures of the specimen propagated across the corners but at a very slow rate, which resulted in a slight strength loss. At the end of the first positive cycle, yielding was more severe, and the fracture on the top side propagated into the flange and widened. The bottom flange fractures were noted as taking place at the end of the second negative cycle. The test continued to finish the third positive cycle. Due to the stroke limitation of the hydraulic actuator, the testing was terminated at end of 0.09-rad TMR before the strength dropped below $0.8M_p$. Major loss of strength was caused by the necking of the corners and large fractures, which progressed nearly across the entire flanges as shown in Fig. 5d. No noticeable LTB, FLB, or WLB was observed.

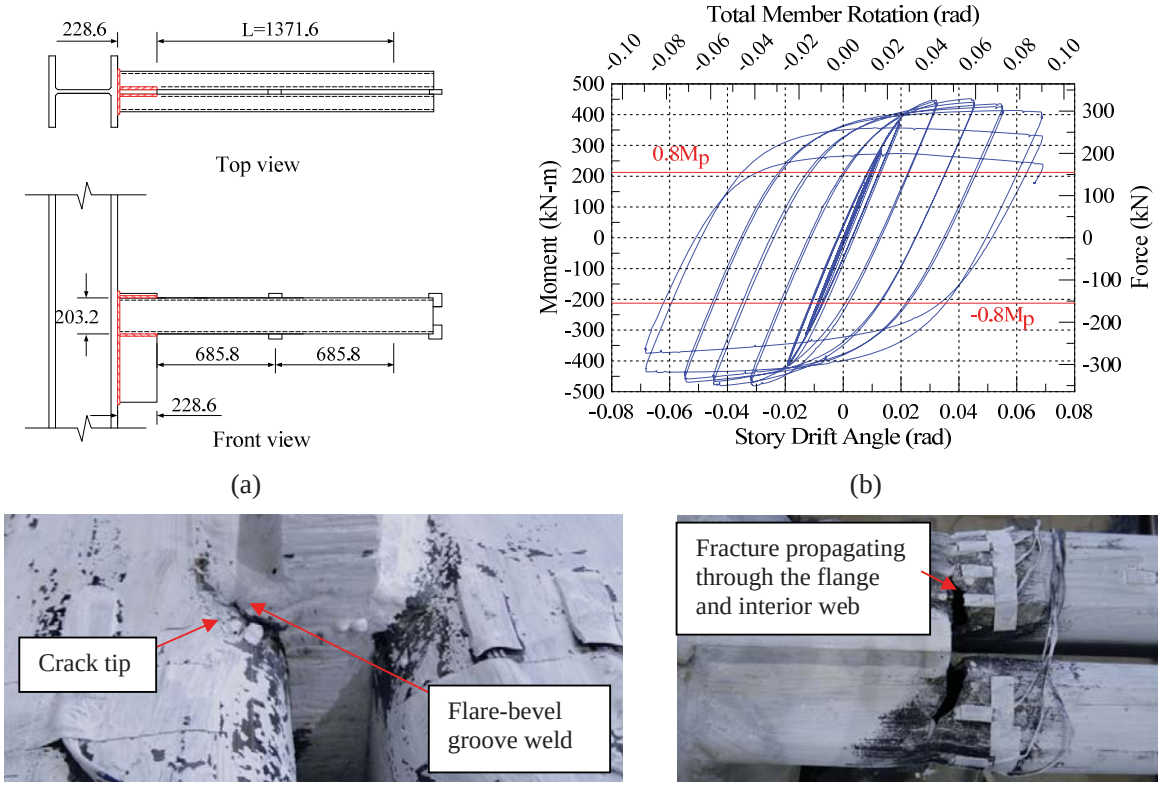

Fig. 5 – (a) specimen details, (b) hysteresis response, (c) fracture at 0.045-rad SDA, and (d) top view of the specimen at the end of the test

2.2 Double-HSS Links

The test setup was designed to simulate the shear and moment diagrams created in the active link of a D-braced EBF where the shear is constant throughout the link but with unequal moments at the two ends. Fig. 6a shows the test setup layout. The test setup had one main column on one side of the double-HSS link and a rigid L-arm on the other side of the double-HSS link. One end of the link was rigidly connected to the main column attached to a stiff H-frame. The other end was connected to a L-arm supported by a stabilizing link. This stabilizing link was able to deform axially, which provided greater rotational flexibility to that end of the link. The rigid L-arm was attached to an actuator and imposed force on the link's mid-span. A lateral bracing system prevented any undesired torsion in the specimen. Fig. 6b shows that the double-HSS link was attached to a gusset plate at each end which connects to an end-plate designed in accordance with the AISC Design Guide 4 [14].

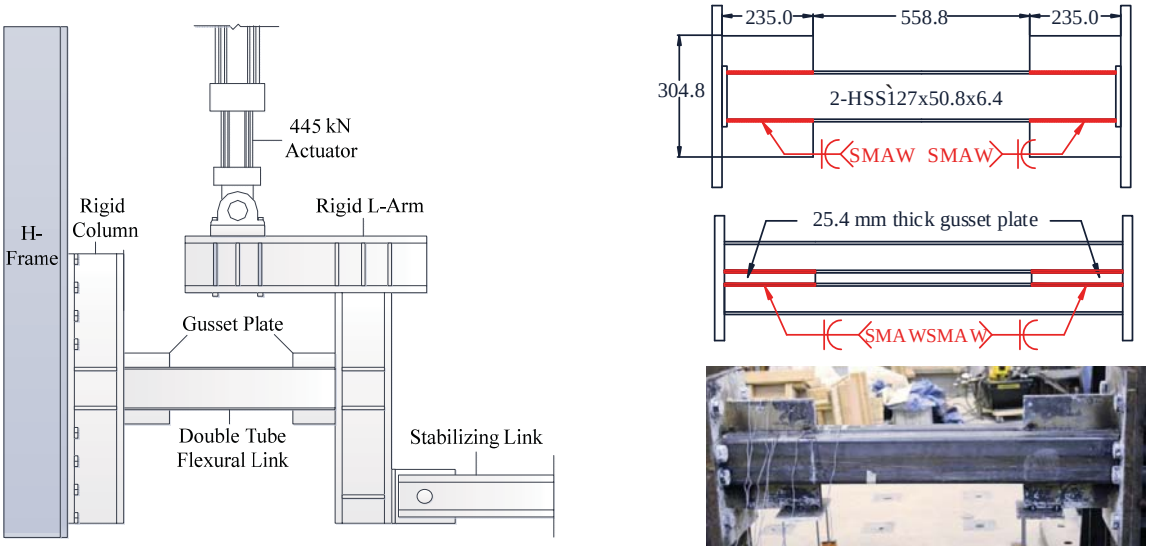

(a) (b)

Fig. 6 – (a) Test setup and (b) link dimensions

The specimen was a 2-HSS127×50.8×6.4 section that was 558.8 mm long (measured from the end of each gusset plate) with an $e/(M_p/V_p)$ ratio of 6.53, where e = 0.5588 m, M_p = 62.0 kN-m, and V_p = 724.6 kN, based on AISC 341 [1], which was well above the 2.6 limit that defines a flexural link. The h/t ratio was slightly above the current threshold for highly ductile members as determined by the AISC 341, 18.5 vs. 16.3, and the b/t ratio was 5.58 [1]. There was a 25 mm thick gusset plate running between the two HSS members that extends 235 mm on either side of the double-HSS specimen. The section was attached to the gusset plate by means of a flare-bevel groove weld along the corner of the double-HSS section. The specimen was tested using the AISC loading protocol [1] for short links.

The specimen reached 11% total rotation angle (9% plastic rotation angle) before excessive loss of the load-carrying capacity. In this case, excessive is defined as the inability to carry 80% of the maximum capacity. A significant fracture appeared in the flange of the specimen as well as in the flare-bevel groove weld at this point during the experiment; nevertheless, the specimen was still able to maintain greater than 80% maximum capacity. The fractures occurred in a ductile manner as opposed to the typical brittle fracture obtained in previous studies, which were performed on wide-flange sections made of A992 steel [15]. The overstrength factor of this specimen was 1.26, which is calculated using $M_u/M_{p(actual)}$ (=78.2 kN-m/62.0 kN-m). This overstrength factor is relatively lower when compared to the overstrength factor of short shear links using a wide-flange section fabricated using A992 steel [11]. The first signs of yielding occurred at the

0.75% total rotation angle as indicated by the strain gauge adjacent to the end of the flare-bevel groove weld. The yielding propagated along the flange and developed into a noticeable plastic hinge on each end of the specimen. The first signs of flange and web buckling occurred at the 9% total rotation angle. A small fracture formed in the tensile flange of the specimen at the end of the gusset plate during the total rotation angle of 11%. During the total rotation angle of 13%, this fracture propagated into the flange, and the load-carrying capacity of the specimen diminished significantly. Fig. 7 shows the specimen at the end of the 15% total rotation angle. At this point, there were significant fractures and buckling prevalent throughout the specimen. The four flanges of the specimen, with the exception of one flange, experienced complete flange fracture that also propagated into the web of the specimen. The one flange, which did not completely fracture, experienced a significant fracture in the flare-bevel groove weld. When the test was stopped, the load being carried at that point was 37% of the maximum capacity of the specimen. Fig. 8 shows the hysteresis loop of the specimen (moment/shear force versus plastic rotation angle). The specimen shows stable results up until 9% plastic rotation angle. The specimen exhibited very stable behavior up to this point with load increasing or remaining essentially constant at every increasing drift step, which allowed the specimen to establish large and full hysteresis loops corresponding to significant energy dissipation.

Fig. 7 – Fracture of link at the end of test (15% total rotation angle or 12% plastic rotation angle)

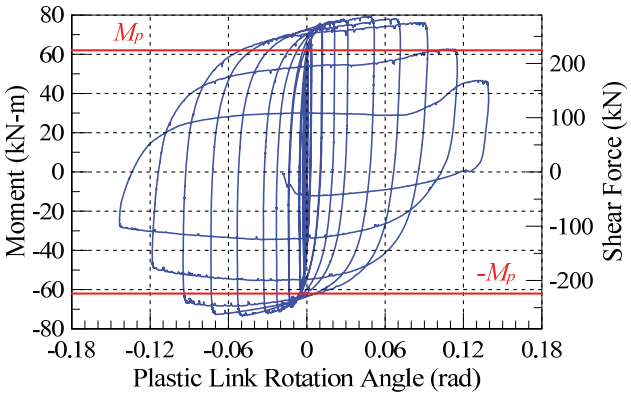

Fig. 8 – Hysteresis loop of double-HSS link

2.3 Double-HSS chord members in special segment of an STMF

A full-scale STMF subassemblage specimen was constructed with double-HSSs (2HSS203.2×101.6×12.7) for chord members (Fig. 4). The vertical members at the ends of the special segment used the same sections as the chord members as suggested by Basha and Goel [16]. The vertical and diagonal members outside of the special segment were also double-HSS built-up sections (2HSS127×127×9.5). The overall length (center-to-center of the columns) was 9695 mm. The length of the special segment was 3025 mm, and the depth of

the truss was 1220 mm. Fig. 9a shows the overall dimensions of the subassemblage specimen. The details of the truss design can be found in [11].

The test setup at the University of Minnesota's Multi-Axial Subassemblage Testing (MAST) Laboratory is shown in Fig. 9b. Stability bracing of the truss was provided, as required by AISC 341 [1], through the truss lateral support system. However, it was located approximately 380 mm outside of the special segment so that it would not obstruct the movement of the specimen when local buckling initiated at the plastic hinges at large story drift ratios. Stability bracing of the truss-to-column connection was provided as per AISC 341 [1] around both columns. Pin connections were used at the top and the bottom of the columns to simulate the inflection points of columns in the multi-story STMF structures. The specimen was cyclically loaded according to a loading protocol similar to the AISC 341 [1] loading sequence for beam-to-column connections of moment frames by means of lateral force applied by the crosshead through a load transfer beam. Details regarding the loading testing procedure can be found in [11] and [12].

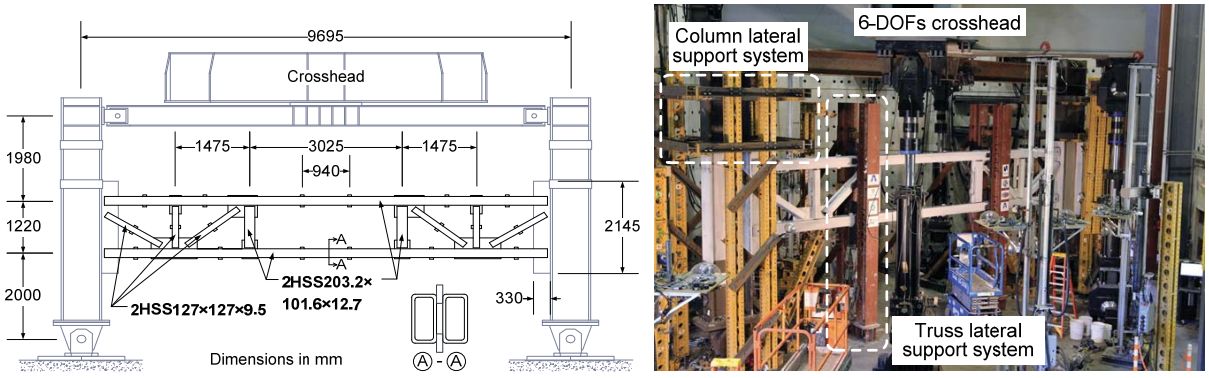

(a) (b)

Fig. 9 – (a) Double-HSS STMF subassemblage overall dimensions (unit: mm) and (b) test setup at MAST

Fig. 10 shows the specimen (special segment) at the end of different story drift ratio cycles. The behavior of the specimen was stable and ductile up to a story drift ratio of approximately 3%. Plastic hinges formed at the expected locations (the ends of the chord members in the special segment) with no yielding in the members outside of the special segment. Figs. 11 and 12 show the members in and outside of the special segment at the end of testing.

As shown in Fig. 13, the specimen behaved elastically up to a story drift ratio of nearly 0.75% and exhibited stable and ductile behavior up to the first cycle of the 3% story drift ratio. Strength increased while stiffness gradually decreased from 1% to 3% story drift ratio. At the end of the first cycle of the 2% story drift ratio, small fractures began to appear at the end of the welds connecting the chord members to the gusset plates at the ends of the special segment; however, they did not affect the overall strength of the specimen. Fractures gradually propagated into the flanges of the chord members at the first cycle of 3% story drift ratio. After the first peak at 3% story drift ratio, large cracks formed on the tension side at the ends of chord members in the special segment and the specimen could not attain the same magnitude of lateral force when it underwent the peak displacement on the opposite direction. The strength dropped slightly during the second cycle of 3% story drift ratio. Specimen strength started to degrade significantly at the first negative cycle of the 4% story drift ratio, at which time the majority of the chord members in the special segment were torn, and the capacity of the specimen drastically dropped to approximately 30% of the peak strength. In the second cycle of 4% story drift ratio, lateral force dropped to about 16% of the peak strength, and the experiment was terminated. Fig. 11 shows the failure at the end of the chord members in the special segment of the subassemblage, which is similar to those of the component test specimens shown in Figs. 5 and 7. In both case, the failure was due to fracturing after low-cycle fatigue accompanied by slight necking of the section. No local buckling and lateral-torsional buckling were observed.

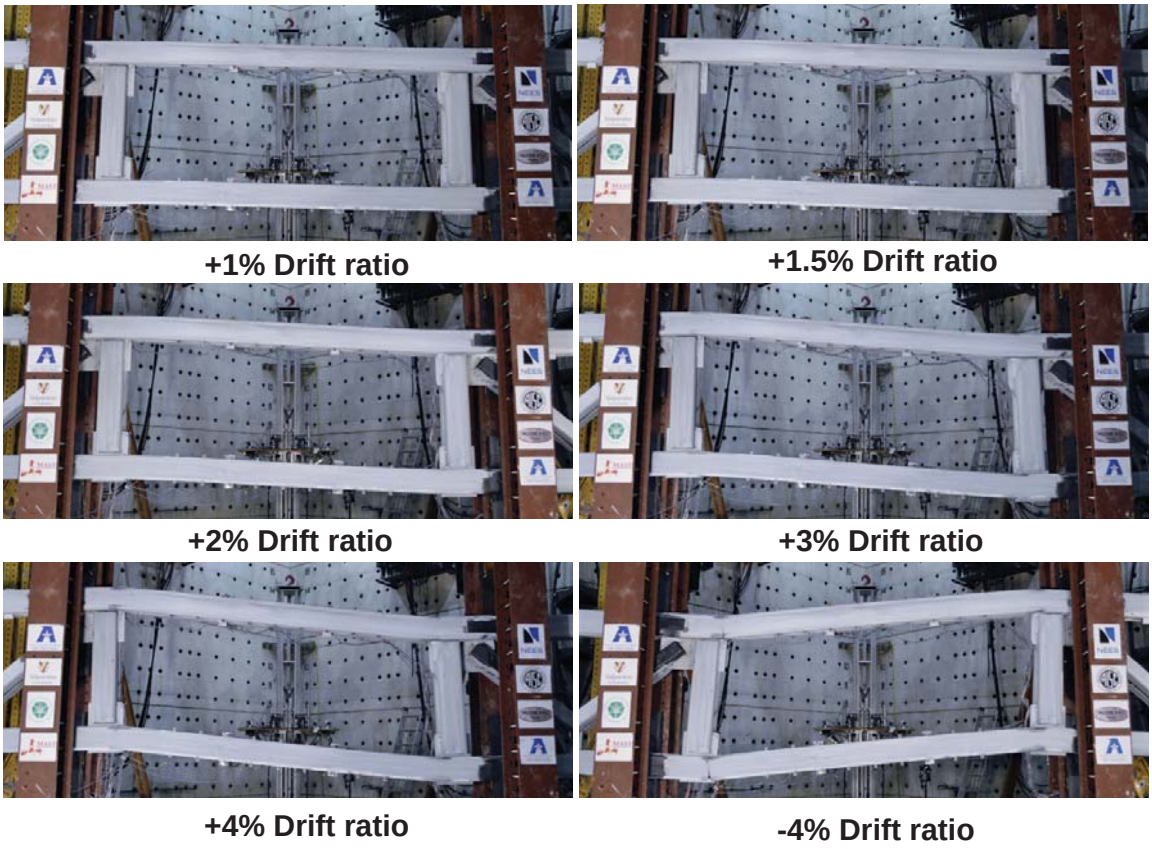

Fig. 1 – Special segment at different drift ratio levels

Fig. 11 – Members in the special segment at the end of testing

Fig. 12 – Members outside of the special segment at the end of testing

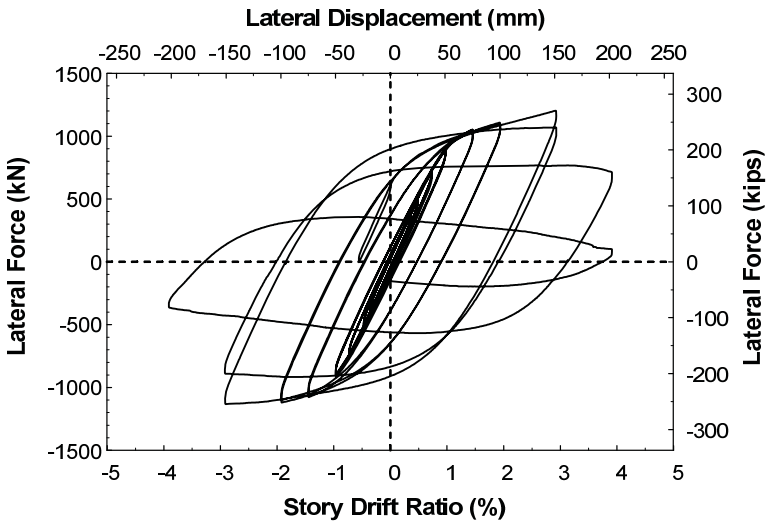

Fig. 13 – Hysteresis response of double-HSS STMF subassemblage

3. Summary and Conclusions

This paper presents several research investigations on exploring the potentials of using the applications of steel double hollow structural section (double-HSS) for seismic resistant members, including moment connections in special moment frames (SMFs), shear links in eccentrically braced frames (EBFs), and chord members in special truss moment frames (STMFs). Hollow structural sections (HSSs) are highly efficient and are used to resist compression, torsion, and bending. Their high torsional rigidity eliminates lateral-torsional buckling (LTB), which also eliminates the need for lateral bracing in beam-type members. As a result, the plastic rotational capacity and strength degradation rate are mainly governed by flange local buckling (FLB) and web local buckling (WLB). The other advantages of using the double-HSS members are: 1) Besides eliminating LTB, it effectively minimizes FLB without increasing the wall thickness by reducing the width-thickness ratio (b/t) with a double-HSS, which significantly enhances the rotational ductility; 2) The gusset plate in-between the two webs also provides support for minimizing WLB; 3) the presence of a gusset plate relocates the plastic hinge away from the column face, which prevents large inelastic strains in the welds between the beam (or link) and the column; 4) They provide simple and economic connection details; 5) They have high shear capacity due to four webs; 6) The welding requirement can be much less stringent since in general only fillet welds are needed.

Double-HSS members used for moment connections in SMFs, links in EBFs, and chord members in STMFs were experimentally assessed. The above advantages and seismic performance of those double-HSS members were experimentally verified by component or full-scale tests. These tests have proven the great potential of using double-HSS members in seismic resistant structures.

4. Acknowledgement

This work was supported in part by the U.S. National Science Foundation (NSF) under Award No. 0936563 and the American Institute of Steel Construction Milek Fellowship.

5. References

[1] AISC. (2016). Seismic Provisions for Structural Steel Buildings, ANSI/AISC 341-16, Chicago, IL.

[2] Nakashima, M., Liu, D., and Kanao, I. (2003): Lateral-Torsional and Local Instability of Steel Beams Subjected to Large Cyclic Loading. *International Journal of Steel Structures*, Vol. 3, No. 3, pp. 179-189.

[3] Uang, C.-M. and Fan, C.-C. (2001): Cyclic Stability Criteria for Steel Moment Connections with Reduced Beam Section. *ASCE Journal of Structural Engineering*, Vol. 127, No. 9, pp. 1021-1027.

[4] Kim, T., Whittaker, A.S., Gilani, A.S.J., and Bertero, V.V. (2002): Experimental Evaluation of Plate-Reinforced Steel Moment-Resisting Connections. *Journal of Structural Engineering*, Vol. 28, No. 4, pp. 483-491.

[5] Okazaki, T., Liu, D., Nakashima, M., and Engelhardt, M. D. (2006): Stability Requirements for Beams in Seismic Steel Moment Frames. *Journal of Structural Engineering*, Vol. 132, No. 9, pp. 1334-1342.

[6] Fadden, M. and McCormick, J. (2012a): Cyclic Quasi-Static Testing of Hollow Structural Section Beam Members. *ASCE Journal of Structural Engineering*, Vol. 138, No. 5, May 2012, pp. 561-570.

[7] Fadden, M., and McCormick, J. (2012b): Effect of Width-Thickness and Depth-Thickness on the Cyclic Flexural Buckling Behavior of Hollow Structural Sections. *Proceedings of the Annual Stability Conference, Structural Research Council*, TX.

[8] D'Aniello, M., Landolfo, R., Piluso, V., and Rizzano, G. (2012): Ultimate Behavior of Steel Beams under Non-uniform Bending. *Journal of Constructional Steel Research*, Vol. 78, pp.144-158.

[9] Chao, S.-H., and Goel, S. C. (2006): A Seismic Design Method for Steel Concentric Braced Frames for Enhanced Performance. *Proceedings, Fourth International Conference on Earthquake Engineering*, Taipei, Taiwan.

[10] Jiansinlapadamrong, C., Simasathien, S., Okazaki, T., and Chao, S.-H. (2017): Cyclic Loading Performance of Full-Scale Special Truss Moment Frame with Innovative Details for High Seismic Activity. *16th World Conference on Earthquake (16WCEE)*, Santiago Chile, January 9 – 13, 2017. Paper N° 2914.

[11] Simasathien, S., Jiansinlapadamrong, C., and Chao, S.-H. (2017): Seismic Behavior of Special Truss Moment Frame with Double Hollow Structural Sections as Chord Members. *Engineering Structures*, Vol. 131, 15 January 2017, pp. 14–27.

[12] Chao, S.-H., Jiansinlapadamrong, C., Simasathien, S., Okazaki, T. (2020): Full-Scale Testing and Design of Special Truss Moment Frames for High Seismic Areas. *ASCE Journal of Structural Engineering*, Vol. 146, No. 3, March 2020.

[13] AISC. (2017). Steel Construction Manual. Fifteenth Edition, Chicago, IL.

[14] Murray, T., and Sumner, E. (2003). Steel Design Guide 4: Extended End-Plate Moment Connections Seismic and Wind Applications, 2nd Ed. American Institute of Steel Construction, Chicago.

[15] Okazaki, T., and Engelhardt, M. D. (2007): Cyclic loading behavior of EBF links constructed of ASTM A992 steel. *Journal of Constructional Steel Research*, Vol. 63, pp. 751–765.

[16] Basha, H. S., and Goel, S. C. (1994): Seismic Resistant Truss Moment Frames with Ductile Vierendeel Segment. Rep. UMCEE 94-29, Dept. of Civil Engineering, Univ. of Michigan, Ann Arbor, MI.

